Hindawi
Journal of Nanomaterials
Volume 2019, Article ID 6316094, 12 pages
https://doi.org/10.1155/2019/6316094

Research Article

Impact of AgNPs on Seed Germination and Seedling Growth: A Focus Study on Its Antibacterial Potential against *Clavibacter michiganensis* subsp. *michiganensis* Infection in *Solanum lycopersicum*

Asma Noshad[1,2] **Crispin Hetherington**[1] **and Mudassar Iqbal**[2]

[1]*Department of Chemistry, nCHREM & Centre for Analysis and Synthesis, Lund University, SE-22100 Lund, Sweden*
[2]*Dept. of Agricultural Chemistry, The University of Agriculture, Peshawar, 25130 KPK, Pakistan*

Correspondence should be addressed to Asma Noshad; asma.noshad@chem.lu.se

Received 23 August 2019; Accepted 29 October 2019; Published 3 December 2019

Guest Editor: Ganga Ram

This study investigated the effect of biogenic AgNPs on seed germination and seedling growth of *Solanum lycopersicum*. Treatment with silver nanoparticles (AgNPs) showed a significantly high germination rate and seedling growth compared to untreated seeds. Furthermore, its bactericidal effect against bacterial pathogen *Clavibacter michiganensis* subsp. *michiganensis* (*cmm*) infection in *Solanum lycopersicum* was also determined. Bacterial canker of tomato (BCT) caused by *cmm* results in reduced plant growth and production leading to considerable economic losses. Herein, fungal extracts of *T. harzianum* and *A. fumigatus* were used separately as a reducing agent to synthesize AgNPs of varying concentrations (0.088 mg/L, 0.176 mg/L, and 0.44 mg/L). Results suggested that the biosynthesized AgNPs not only worked as bactericide but also completely inhibited the incidence of *cmm* infection even at the lowest concentration of 0.088 mg/L under greenhouse conditions. Plants treated with AgNPs showed significantly enhanced growth parameters including plant height (cm), tomato yield/plant (g), fresh biomass (g), number of shoots/plant, root weight (g), and dry biomass (g). So, in order to reduce the toxic effects of chemical-based bactericides, biobased AgNPs are recommended, not only to control but also to prevent the bacterial infection in agriculture.

1. Introduction

Large doses of conventional chemical pesticides have resulted in the development of pest resistance and environmental contamination which are becoming one of the big challenges in agricultural industry. It has compelled research organizations to search for effective alternate (both in terms of cost and performance) plant protection pesticides. Integration of metal-based nanoparticles (NPs) in agriculture should be compatible with these requisites as they offer more efficient and eco-friendly alternates to conventional agricultural practices, e.g., nanopesticides, nanofertilizers, and nanosensors [1, 2]. Emergence of biobased nanopesticides which have a slow release formulation and are able to degrade active ingredients slowly proposes a hope of a more eco-friendly replacement to the chemical pesticides [3, 4]. In particular, fungal-based AgNPs could be the most feasible option due to their excellent antimicrobial potential for most of biomedical and industrial applications [4–6]. The focus of this study is to utilize beneficial fungi as they have several advantages over other microbes for many reasons; e.g., enzymes secreted by fungi play an important role in the synthesis of silver nanoparticles because of their ability to work both as reducing and stabilizing agents, but the detailed mechanism is still to be elucidated [7]. Previous studies highly recommend *A. fumigatus* for rapid biosynthesis of AgNPs effective against bacterial pathogens [8, 9]. Though the mechanism behind it is not yet well known, there exists a generally accepted mechanism. Extensive research needs to be carried out to conclude and generalize it.

Among the microbial syntheses of AgNPs, fungi are preferred due to

(i) excellent secretion of extracellular enzymes resulting in faster fabrication of AgNPs than chemical synthesis

(ii) involvement of NP synthesis in a cost- and time-effective manner

(iii) ease in isolating, culturing, processing, and storage

(iv) successful involvement in high-yield economy NPs

(v) nanoparticles by fungi being more stable with better monodisparity [7]

Myco-based fabrication of metal NPs is getting much research interest due to their extensive application in various sectors (Table 1).

This study was designed to synthesize and characterize AgNPs using 2 different fungal strains which is an economical, harmless, eco-friendly, and acceptable method. The fungal strains used were *T. harzianum* [11] and *A. fumigatus*. The biosynthesized AgNPs were subjected to *in vitro* screening for antibacterial efficacy against Gram-positive and Gram-negative bacteria. Based on the excellent outcome of *in vitro* antimicrobial potential, a greenhouse experiment was conducted to determine the effect of treatments on a control of *Clavibacter michiganensis* subsp. *michiganensis*. *cmm* is a bacterial pathogen responsible for bacterial canker of tomato (BCT) [20, 21] and a major production restraint, causing significant economic losses worldwide. Various biotic and abiotic stress factors contribute to this low yield; however, this study is focused on one of the biotic stress factors known as BCT. Lack of conventional resistance in tomato cultivars has made it very difficult to control it. So, the overarching aim of this study is to develop AgNPs through the green chemistry route with the ambition that these particles contribute some beneficial effects to the industrial agriculture in preventing and treating BCT. The synthesized AgNPs were characterized by UV-visible absorption spectra and X-ray diffraction (XRD) and confirmed by transmission electron microscope (TEM). The effect of pH on AgNPs during synthesis process and its stability behavior for six months were also kept under observation. It was also determined if the reduction process is an enzymatic reaction. Though it is not the first report to employ filamentous fungi *A. fumigatus* and *T. harzianum* for the extracellular synthesis of AgNPs, they are used for the first time to control the bacterial pathogen *cmm* which is considered under quarantine in Europe but still prevalent in many developing and underdeveloped countries. The production of antimicrobial compounds by the fungi *P. oligandrum* and *T. harzianum* highlights its importance [22].

2. Experimental

2.1. Isolation and Culturing. Pure cultures of *A. fumigatus* and *T. harzianum* were collected and reidentified at the Plant Pathology Dept. of the University of Agriculture, Peshawar. The obtained cultures were inoculated and grown using the protocol described by [11]. The experimental steps involved are as follows:

(i) Collection of fungal strains

(ii) Cultured or grown on nutrient medium

(iii) Exposure of the fungal filtrate solution to silver nitrate solution for the biosynthesis of AgNPs

(iv) Characterization process includes UV-Vis spectroscopy, TEM, energy-dispersive X-ray spectroscopy (EDX), and powder PXRD analysis

(v) *In vitro* antibacterial activity

(vi) Stability test for the synthesized AgNPs

(vii) Mechanism behind enzymatic reaction of AgNP synthesis

(viii) Effect of pH on AgNP synthesis

(ix) Seed germination and seedling growth test

(x) Screenhouse experiment to check the effect of synthesized AgNPs on *cmm* subsp. *michiganensis* control

2.2. Statistical Analysis. Origin Professional 8 (Microsoft, USA) software was used for statistical Gaussian approximation to find the full width at half maximum (FWHM). A completely randomized design CRD with 3 replications was used for the experiment. Calculation of one-way ANOVA, P value < 0.05 is considered statistically significant.

The experimental steps involved in AgNP synthesis using the fungal source, their characterization, and antibacterial application *in vitro* as well in the greenhouse is presented in Figure 1. The explanation for each step is described with results in brief.

3. Results and Discussion

3.1. Synthesis of AgNPs. The prepared filtrate of each fungal isolate was brought in contact with $AgNO_3$ in 1 : 1 at 29°C. A robust colour change from yellow to brown was observed after 24 hours of the incubation period, indicating AgNP formation (Figures 2(a) and 2(b)). A sharp characteristic peak centered at ca. 422-429 nm and 425-4439 nm due to surface plasmon resonance SPR value in the visible region of the spectrum for *T. harzianum* and *A. fumigatus*, respectively (Figure 3). Increase in SPR value towards higher wavelength is proportional to the intensity of Ag in the reaction mixture, resulting in an increased number of AgNPs in the solution w.r.t. time [23]. The mechanism behind the synthesis of AgNPs involved bioreduction of silver ions to metallic silver (Ag^{+2} to Ag^{0}), later on stabilized by the bioactive molecules present in the mycelial cells. During this process, toxic metal ions Ag^{+2} are reduced to nontoxic AgNPs through the catalytic effect of the extracellular enzyme and metabolites secreted by fungi [24]. No colour change was observed in the control experiment when incubated under the same conditions (Figure 3). However, to justify that fungus-mediated AgNPs are the result of an enzymatic reaction, each of the fungal filtrate was boiled for 15 minutes to denature the proteins secreted by the fungi. This filtrate was used in the same

Table 1: Applications of AgNPs synthesized from different fungal strains.

Nanoparticles	Fungi/yeasts	Application	References
Ag	*A. niger*	Antibacterial activity, wound healing activity	[8]
	Fusarium acuminatum	Antibacterial properties against multidrug-resistant bacteria	[9]
	F. oxysporum	(i) Textile fabrics (ii) Antibacterial properties against multidrug-resistant bacteria	[10]
	Trichoderma harzianum	Antibacterial properties against multidrug-resistant bacteria	[11]
	Rhizopus stolonifer	Antifungal activity	[12]
	Penicillium oxalicum	Catalytic activity	
	Penicillium sp.	Antibacterial activity against MDR	[13]
	F. solani	Antibacterial effect by fungal process on cotton fabric	[14]
	Pleurotus ostreatus, *P. florida*, and *P. citrinopileatus*	Antimicrobial activity	[15]
	Alternaria alternata	Antifungal activity	[16]
	A. clavatus	Antimicrobial activity	
	T. viride	Vegetable and fruit preservation	[18]
	Penicillium sp.	Antibacterial properties against multidrug-resistant bacteria	[19]

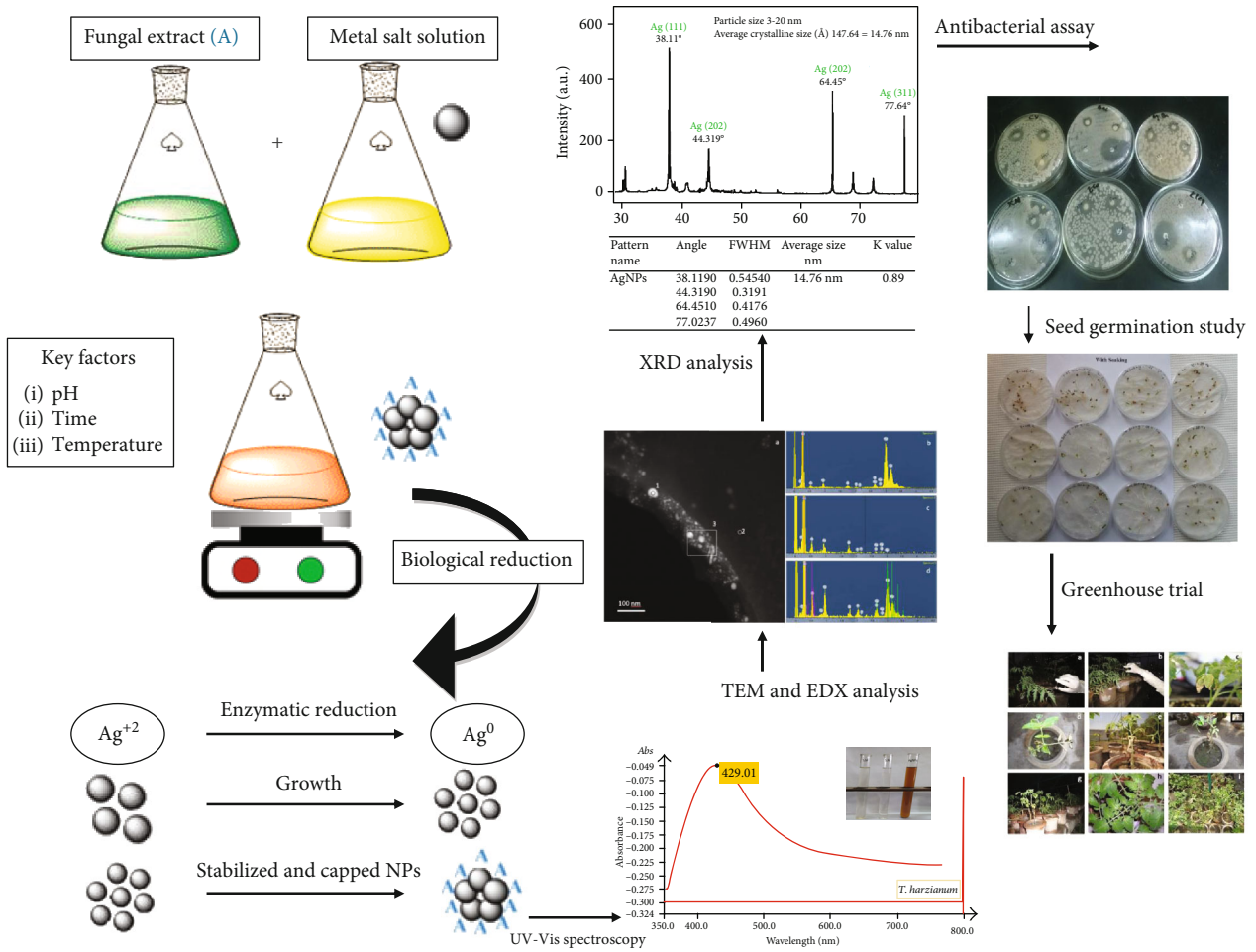

Figure 1: Graphical representation of experimental steps involved in the biological synthesis of AgNPs, characterization, and application.

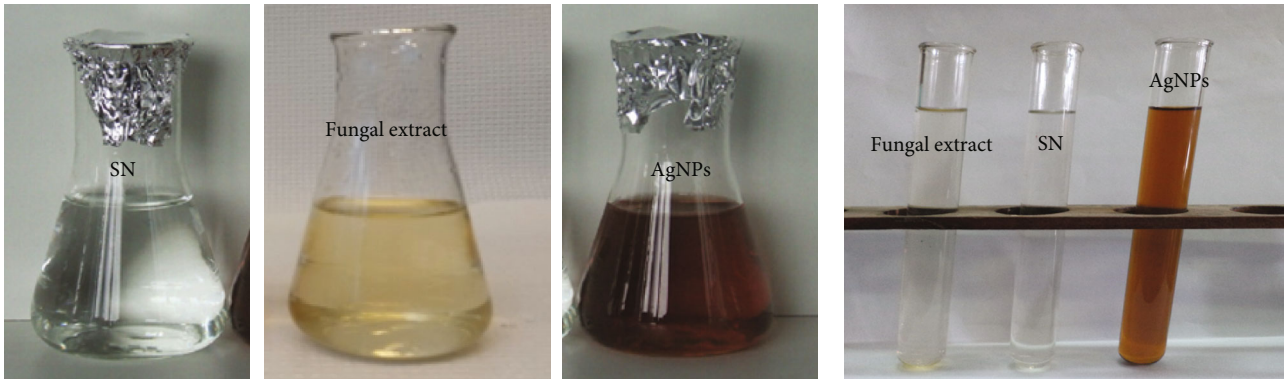

Figure 2: Colour change from yellowish to dark brown after incubation signifying AgNPs formation. (a) fungla extract of *T. harzianum* treated with silver nitrate solution (SN) resulting in the formation of AgNPs (images reproduced with permission from Ref. [11]]. (b) fungla extract of *A. fumigatus* treated with silver nitrate solution (SN) resulting in the formation of *A. fumigatus*-mediated AgNPs.

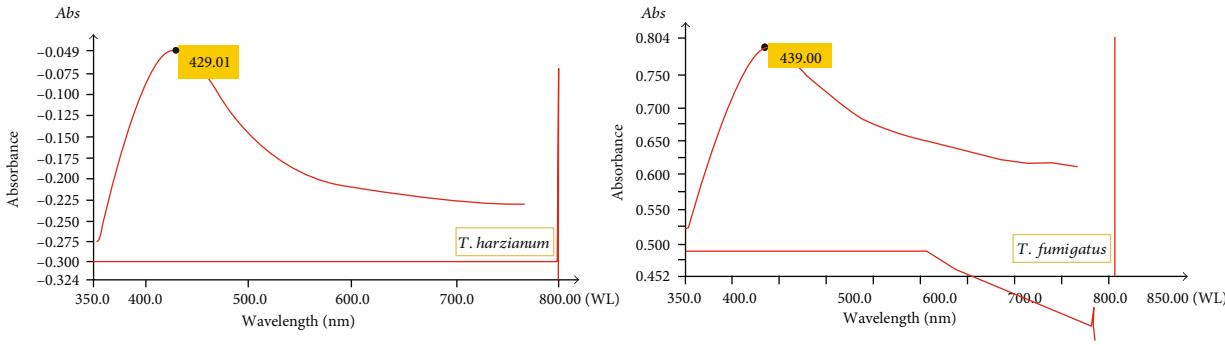

Figure 3: UV spectra for the solution mixture of fungal extract of *T. harzianum* and *A. fumigatus* mixed with $AgNO_3$ salt, showing absorbance peaks at 429.01 and 439 nm, respectively, while the downwards straight line indicates the UV spectrum for the boiled fungal extracts mixed with $AgNO_3$ salt, showing no absorbance peak for AgNPs, supporting the hypothesis of enzyme-based biosynthesis of AgNPs.

way as stated above for AgNP synthesis resulting in no colour change. The resultant reaction mixture was further confirmed for AgNP synthesis by a comparison of its spectra before and after its exposure to fungi as shown in Figure 3. The absorbance spectra for the reaction mixture showed no absorbance confirming that enzymes secreted from fungi are responsible for reducing Ag^+ into AgNPs. After the completion of the reaction, the solution was centrifuged at 10,000 rpm for 15 min, the supernatant was separated, and the settled material was dried under reduced pressure to obtain a solid material for characterization purposes.

3.2. Stability Test. To check the stability of the reaction mixture, it was kept at room temperature for six months and the absorption was monitored regularly. Our results confirmed that the solution mixture remains highly stable for six months with no evidence of aggregation of particles.

4. Effect of pH

Increase in pH has been observed for both samples until a stable SPR peak has been attained using UV-Vis spectroscopy as listed in Table 2. There was no noticeable change in the SPR value of the reaction mixture after 24 hours of the reaction demonstrating that the reaction came to equilibrium. Under low pH value, a pale white and yellow colour was observed which turned into dark brown with successive increase in pH of the reaction [25, 26]. Production of smaller and regular round-shaped AgNPs has been observed under high pH > 10 [26]. The pH values for the synthesized AgNPs on the selected PDB media were found to be in the range of 8.5-11.0.

For further details into the morphology and size of AgNPs, few drops of liquid suspension was coated on a carbon-coated copper grid and allowed to dry. The grid was then scanned employing HRTEM (JEOL 3000F). The obtained TEM image for AgNPs from both fungal samples displayed well-dispersed round-shaped AgNPs of 3-20 nm and 4-20 nm in size, respectively (Figures 4 and 5). TEM images revealed formation on the highest amount of AgNPs for *A. fumigatus* which is in agreement with the high intensity of the SPR value obtained for *A. fumigatus* also correlating with the earlier report of [27]. Thus, fungal species *A. fumigatus* is highly recommended for industrial-scale production of AgNPs. Energy-dispersive X-ray (EDX) analysis for both samples showed a high amount of AgNPs in the silver region confirming complete reduction of Ag^+ into AgNPs (Figures 4 and 5). Besides Ag, other weak signals for elements

Table 2: Presenting change in pH values along with UV-Vis peak data for the biogenic AgNPs from *T. harzianum* and *A. fumigatus*.

Source	Reduction time	UV-Vis peak (nm)	Colour change	pH change
T. harzianum	6-24	422-429	Pale yellow-dark brown	8.8-10.2
A. fumigatus	24	425-439	Light yellow→dark brown	8.0-11.5

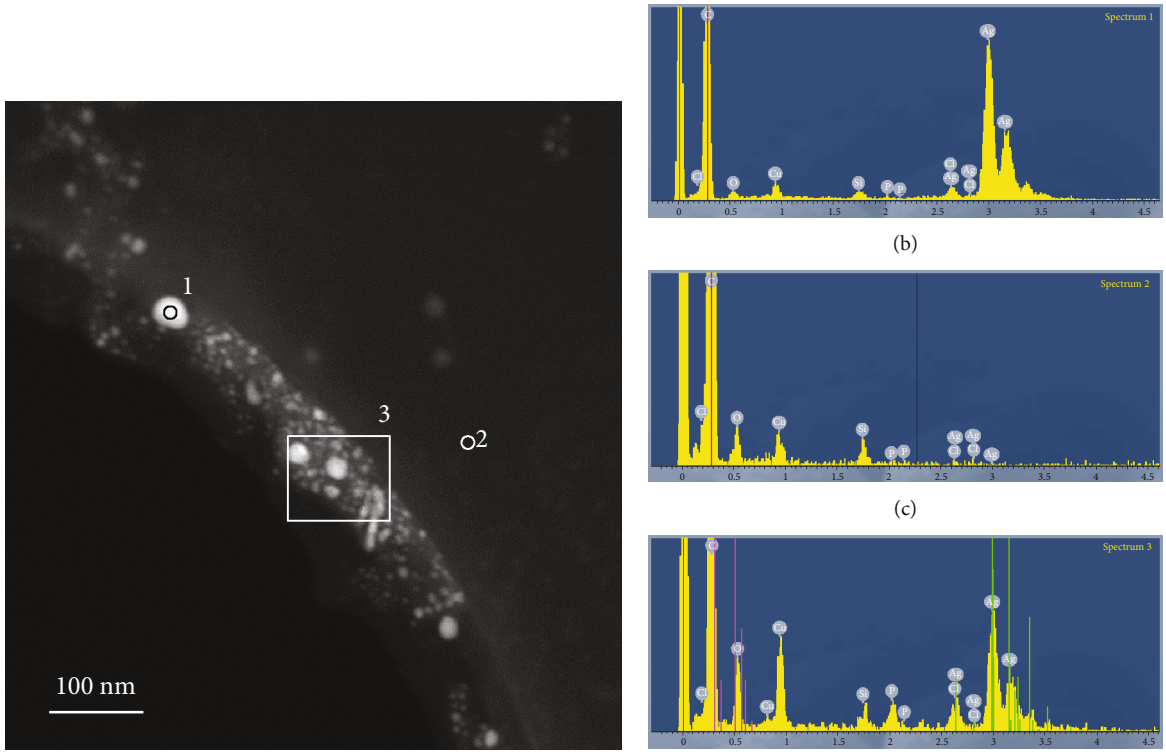

Figure 4: STEM micrograph (a) of AgNPs obtained from the fungal mycelium of *T. harzianum* challenged with $AgNO_3$ solution and EDX spectra (b–d) from 3 areas. The EDX spectrum from area 3 is shown in (d) with green lines indicating positions of peaks for Ag. These lines are absent in the spectrum in (c) which is taken from the support film (figure reproduced with permission from Ref. [11]].

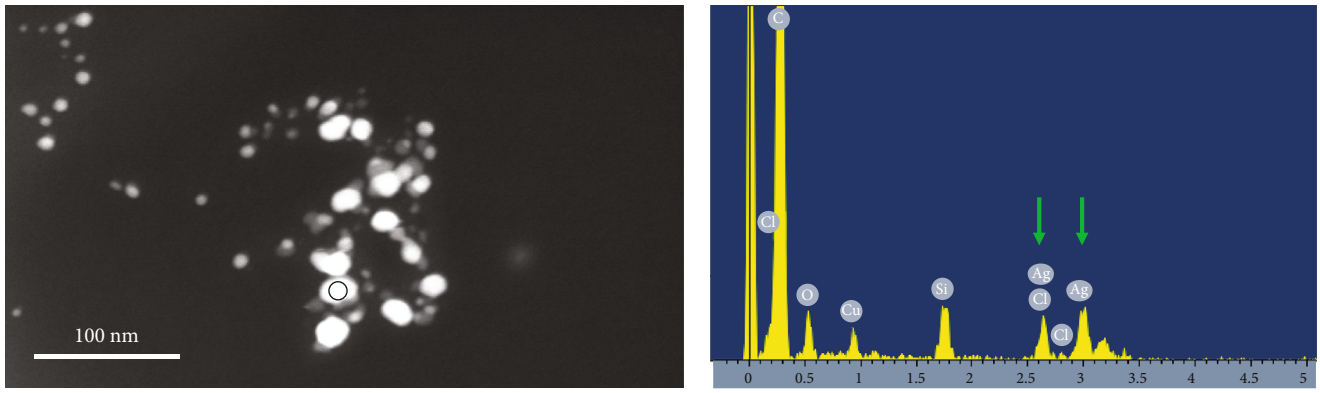

Figure 5: STEM micrograph (a) of AgNPs from *A. fumigatus*. The circle on a nanoparticle indicates the location from which the EDX spectrum was taken (b). Green arrows point to the peaks at the energies (in keV) corresponding to Ag. Other peaks come from the support film and grid.

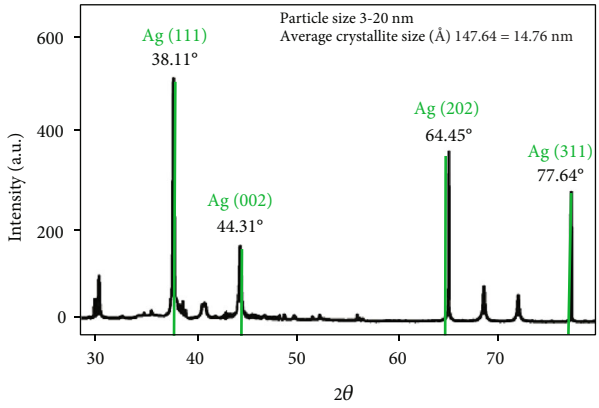

Pattern name	Angle	FWHM	Average size (nm)	*K* value
AgNPs	38.1190	0.5454	14.76 nm	0.89
	44.3190	0.3191		
	64.4510	0.4176		
	78.0237	0.4960		

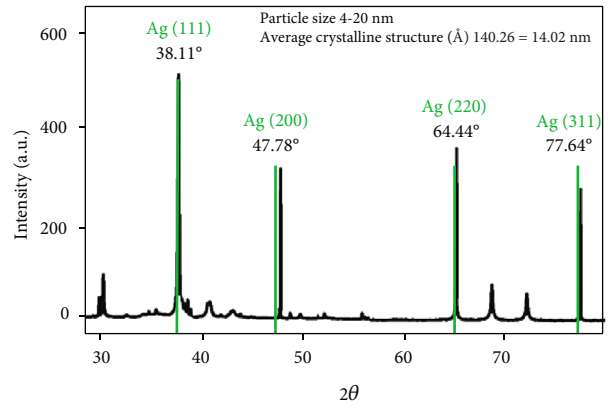

Pattern name	Angle	FWHM	Average size (nm)	*K* value
AgNPs	38.1148	0.3578	14.02 nm	0.89
	47.7831	0.4147		
	64.4435	0.3348		
	77.6438	0.4278		

FIGURE 6: X-ray diffraction data for AgNPs fabricated from the reaction mixture of the $AgNO_3$ salt solution and fungal extract of *T. harzianum* and *A. fumigatus*.

including C, Cu, O, and Si were also identified due to the carbon-coated copper TEM grid used for sample deposition. SEAD measurements signify that the extracellular synthesis of AgNPs by *T. harzianum* and *A. fumigatus* produces highly crystalline AgNPs which is also in agreement with the XRD peak data.

The biosynthesized metal NPs were subjected to PXRD analysis for qualitative measurement (phase variety and crystal structure) using PXRD (STOE Stadi MP). XRD pattern for the synthesized AgNPs was recorded in a wide selection of Bragg angles 2θ (30 to 80) operated at a voltage of 40 kV and current of 40 mA with a scan rate of 0.01°/s. The identified silver peaks were quite intense and comparably very sharp, indicating a high face-centered cubic (fcc) crystal structure of the AgNPs. X-ray diffraction peaks correspond to the (111) (002) (202) (311) and (111) (200) (220) (311) sets of lattice planes (Figure 6). The coherently diffracting crystallography domain sizes of 14.76 nm and 14.02 nm of the AgNPs are calculated from the width of the XRD peaks using the Scherrer formula [28]. Thus, the current XRD data infers that AgNPs synthesized from fungi could be effectively utilized for the green synthesis of round-shaped, crystal-structured, and well-defined dimension AgNPs.

5. Antimicrobial Effect of Biosynthesized AgNPs

The antibacterial assay of biogenic AgNPs was conducted using standard disc diffusion assay on nutrient agar media described by Noshad et al. [11]. The antibacterial potential for fungal-based AgNPs was evaluated against six bacterial strains including G+ve (*E. coli*, *Agrobacterium tumefaciens*, and *Xanthomonas campestris*) and G-ve (*Clavibacter michiganensis* subsp. *michiganensis*, *Streptococcus thermophilus*, and *Bacillus subtilis*). The synthesized AgNPs were applied in two different concentrations. A comparative study for AgNPs was made with $AgNO_3$ as the negative control and streptomycin solution as the positive control. The inoculated plates were incubated at 37°C for 24 h, and the inhibition zones were calculated using a caliper. All the experiments were carried out in triplicate recorded as the mean standard error (±SE). Compared to control treatments, excellent antimicrobial effect was observed for both samples (AgNPs) (Tables 3(a) and 3(b)). The synthesized biogenic AgNPs completely inhibited bacterial growth at all treated concentrations of 0.088 mg/L, 0.176 mg/L, and 0.44 mg/L. In Figures 7 and 8, it can be observed that the inhibition zones produced by AgNPs are comparable to a standard antibiotic (streptomycin) while being larger than the inhibition zones of control treatments, i.e., SN. Compared to bulk Ag, AgNPs possessed unique biological and physiochemical properties, making them the ideal antibacterial agent. Though the exact antibacterial mechanism of action is yet not understood, there exists a generally accepted mechanism, i.e., through release of Ag^+. Many reports suggested the importance of Ag^+ in enhanced antibacterial effect [29–32]. There exists a direct relation of the AgNP surface area to released Ag^+ concentration. AgNPs of the highest surface area will release the highest concentration of Ag^+ and vice versa. When AgNPs interact with a bacterial cell, they bind to the proteins in the cell membrane and penetrate into the cell. The released Ag^+ interacts with cellular structures such as respiratory enzymes and releases reactive oxygen species (ROS) resulting in apoptosis like DNA damage and cell death [33, 34].

Furthermore, it was also observed that the antimicrobial effect for both samples (AgNPs) was stronger against *cmm* subsp. *michiganensis*. So a greenhouse trial was planned to check the effect of AgNPs on the *cmm* control. For this purpose, a seed germination test was carried out first in the laboratory condition to see the impact of AgNPs on the seed germination rate, though several studies have reported varied influence of NPs on seed germination and root growth. For example, AgNPs had positive impact on the germination rate

Table 3

(a) Represents measurement for zone of inhibition (mm) for AgNPs from fungal filtrate of *A. fumigatus* against the listed microbial pathogens and comparative studies with different controls including streptomycin as the standard and silver nitrate (SN) as the blank

Indicator bacteria	Zone of inhibition (mm ± SE)				
	Streptomycin	AgNP			$AgNO_3$
		0.088 mg/L/disk	0.176 mg/L/disk	0.44 mg/L/disk	
C. michiganensis	1.16 ± 0.13	1.10 ± 0.10	1.14 ± 0.10	1.15 ± 0.10	0.86 ± 0.08
X. campestris	1.16 ± 0.13	0.96 ± 0.08	1.10 ± 0.10	1.10 ± 0.13	0.86 ± 0.08
E. coli	1.25 ± 0.10	1.06 ± 0.03	1.10 ± 0.08	1.10 ± 0.00	0.86 ± 0.08
S. thermophilus	1.36 ± 0.10	1.03 ± 0.13	1.03 ± 0.10	1.03 ± 0.11	0.86 ± 0.08
Ag. tumefaciens	1.13 ± 0.11	1.02 ± 0.05	1.06 ± 0.10	1.06 ± 0.08	0.86 ± 0.08
B. subtilis	1.26 ± 0.10	1.18 ± 0.10	1.20 ± 0.10	1.22 ± 0.03	0.86 ± 0.08

(b) Represents measurement for zone of inhibition (mm) for *T. harzianum*-mediated AgNPs against the listed microbial pathogens

Indicator bacteria	Zone of inhibition (mm ± SE)				
	Streptomycin	AgNP			$AgNO_3$
		0.088 mg/L/disk	0.176 mg/L/disk	0.44 mg/L/disk	
C. michiganensis	1.16 ± 0.13	0.93 ± 0.08	1.12 ± 0.08	1.16 ± 0.08	0.80 ± 0.01
X. campestris	1.12 ± 0.10	0.96 ± 0.12	1.06 ± 0.11	1.10 ± 0.08	0.80 ± 0.01
E. coli	1.46 ± 0.11	1.03 ± 0.08	1.16 ± 0.11	1.39 ± 0.08	0.80 ± 0.01
S. thermophilus	1.36 ± 0.03	1.08 ± 0.02	1.08 ± 0.03	1.30 ± 0.08	0.80 ± 0.01
Ag. tumefaciens	1.06 ± 0.08	0.73 ± 0.08	0.73 ± 0.08	1.00 ± 0.08	0.80 ± 0.01
B. subtilis	2.25 ± 0.03	1.26 ± 0.12	1.26 ± 0.03	2.15 ± 0.08	0.80 ± 0.01

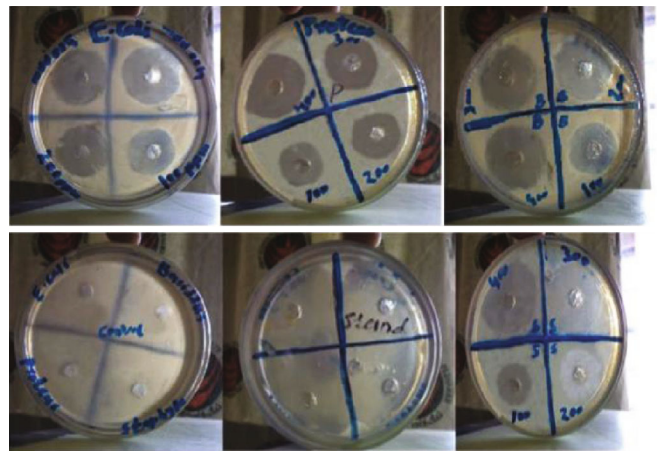

Figure 7: Antibacterial activity of biologically synthesized AgNPs from *T. harzianum* against G+ve (*E. coli, Agrobacterium tumefaciens*, and *Xanthomonas campestris*) and G-ve (*Clavibacter michiganensis* subsp. *michiganensis*, *Streptococcus thermophilus*, and *Bacillus subtilis*).

and seedling growth of *Pennisetum glaucum* [35]. TiO_2 NPs increased the seed germination rate of funnel seeds, and the same effect has been reported for ZnO NPs in cucumber [36]. In the case of corn, barley, and soybean, an enhanced germination rate has been documented using CNTs [36], though CNTs pose reduced seed germination in *L. sativum* [35]. Meanwhile, other investigations reported negative impact of CuO-based NPs on the seed germination rate of rice [37] while it had no effect on the seed germination rate of maize [38].

Results suggested that *S. lycopersicum* seeds treated with AgNPs resulted in a higher number of sprouted seeds in 3 to 12 days of germination, while in control treatments, the same effect has been observed on 14 to 18 days (Figure 9). Furthermore, compared to control treatments, increased length has been observed for AgNP-treated seedlings

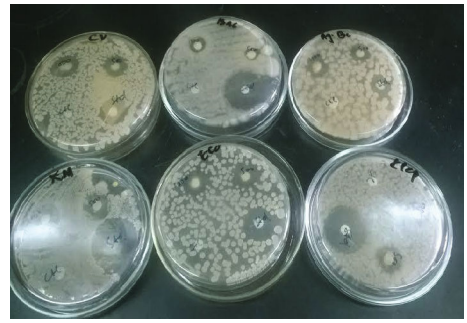

Figure 8: Antibacterial activity of biologically synthesized AgNPs from *A. fumigatus* against the Gram-positive and Gram-negative bacteria mentioned in Figure 7.

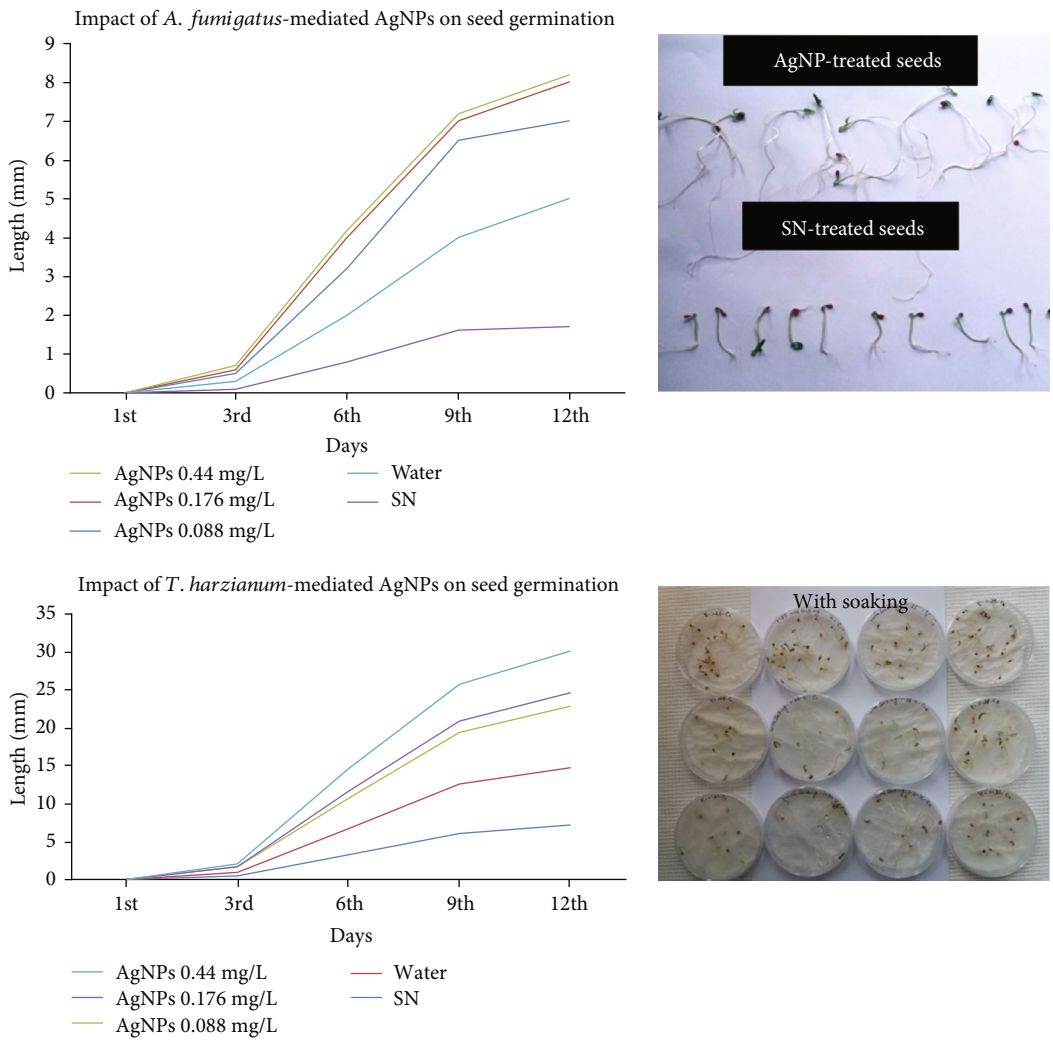

Figure 9: Graphical presentation for the impact of synthesized AgNPs on seed germination and seed growth. Panel (a) represents *A. fumigatus*-made AgNPs while (b) is for *T. harzianum*-made AgNPs. The inserted images (c) clearly demonstrate increased seedling length for AgNP-treated seedlings.

(Figure 9). The possible reason behind the enhanced seedling growth rate could be the efficient water and nutrient uptake by the treated seeds as AgNPs can penetrate through the seed coat and may activate the embryo. During penetration, AgNPs cause more new pores that remain helpful in carrying nutrients, efficiently leading to fast germination and growth rate [39]. $AgNO_3$ solution resulted in reduction in all observed growth parameters suggesting the toxic behavior

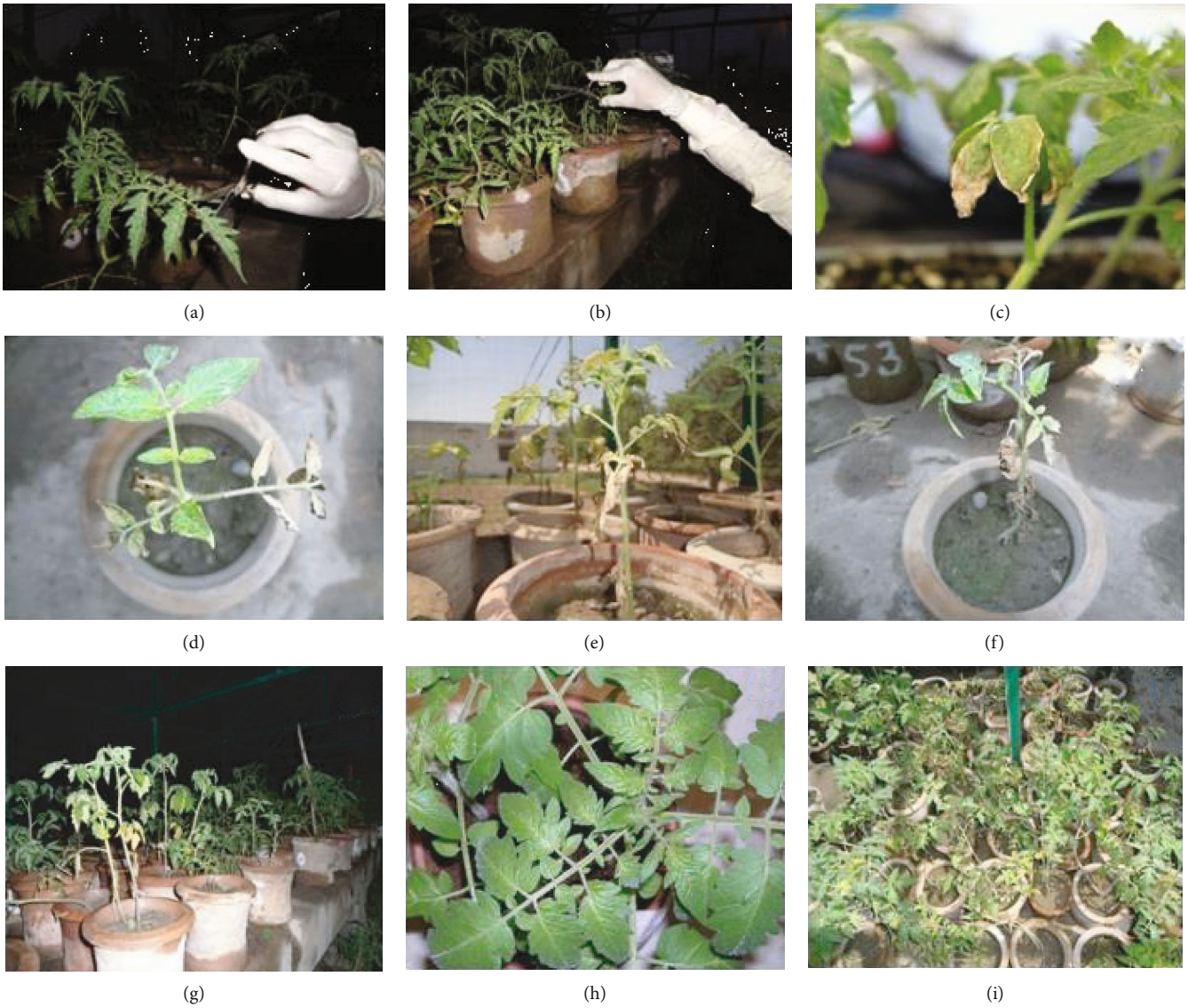

Figure 10: (a, b) shows inoculation of 6-week-old plants of tomato with *cmm* culture. (c, d) represents symptoms of BCT infection on tomato leaves upon artificial inoculation of *cmm*—appeared in control treatments only. (e, f) represents $AgNO_3$-treated plants—symptoms appeared and reduced growth of plants was also observed. Normal healthy growth was observed for AgNP-treated plants (g–i).

of a higher concentration of ionic silver to the plants, whereas only fungal extract had no measurable effect on the germination rate of *S. lycopersicum* seeds. It can be assumed here that stability of AgNPs with the fungal extract might be responsible for reducing its toxicity, also supported by [40]. The obtained outcome could be helpful to enhance the seed germination rate and seedling growth especially in dormant seeds. 6-week-old plants were transplanted (1 seedling/pot) to 15 cm diameter earthen pots. Each pot had 2 kg of standard commercial mix with slow release fertilizer. Different doses, i.e., 0.088 mg/L, 0.176 mg/L, and 0.44 mg/L, of AgNPs were mixed with the soil before transplanting seedlings. All of the plants were inoculated by clipping 3 inoculation sites per plant including 1 shoot per plant and the 2 youngest actively growing leaves per shoot and middle stem with scissors that had been dipped into *cmm* suspension. On the 7^{th} week of the plant growth, plants were exposed to AgNPs weekly, once the symptoms appeared. Results demonstrated that compared to the control treatment, the biosynthesized AgNPs inhibited the growth of *cmm* completely (Figure 10). Importantly, application of the $AgNO_3$ solution alone resulted in reduced growth of plants which highly supports our assumption that the stability of AgNPs with the fungal extract might be responsible for reducing its toxicity in agreement with [40]. Compared to the control, all of the plant growth parameters including plant height (cm), tomato yield/plant (g), plant fresh biomass (g), number of shoots/plant, and plant dry biomass (g) showed significant healthy growth supporting the beneficial effect of biogenic AgNPs against the harmful effects of the bacterial pathogen *cmm* (Table 4).The

Table 4: Impact of AgNPs on disease incidence %, plant height, fresh biomass, dry biomass, and shoot per plant grown under screenhouse conditions.

	Treatment	Plant height	Fresh biomass	Dry biomass	Shoot/plant	D.I.%
T. harzianum-made AgNPs	0.088 mg/L	65.2 ± 0.36	355.38 ± 1.26	76.79 ± 0.31	5.5 ± 0.33	31.47
	0.176 mg/L	68.0 ± 0.33	375.32 ± 1.30	88.83 ± 0.39	6.0 ± 0.23	25.50
	0.44 mg/L	72.8 ± 0.27	380.28 ± 0.91	90.07 ± 0.19	7.2 ± 0.23	22.61
A. fumigatus-made AgNPs	0.088 mg/L	62.4 ± 0.69	360.00 ± 0.97	85.66 ± 0.45	5.8 ± 0.43	9.52
	0.176 mg/L	64.6 ± 0.80	372.00 ± 0.91	90.30 ± 0.48	6.0 ± 0.27	7.14
	0.44 mg/L	65.0 ± 0.33	382.80 ± 0.49	92.40 ± 0.43	7.5 ± 0.06	5.95
	Streptomycin	72.8 ± 0.79	381.60 ± 0.90	95.20 ± 0.72	7.6 ± 0.18	6
	SN	39.0 ± 0.66	105.20 ± 0.76	39.50 ± 0.51	2.4 ± 0.18	100
	Water	36.8 ± 0.27	159.40 ± 0.64	27.88 ± 0.31	2.4 ± 0.18	100

in vitro and screenhouse experiments remain successful against BCT control and showed a similar pattern of results as observed in seed germination and seedling growth.

6. Conclusion

Due to the antibiotic resistance profile, multidrug-resistant bacteria are developing which is becoming a severe problem. Use of broad-spectrum antibiotics to control it is more toxic, less effective, and more expensive [41]. So the researchers are attracted towards AgNPs, as there is much evidence suggesting that the use Ag^+ in the form AgNPs enhances the antibacterial activity many folds [42]. Thus, the results presented in this study are novel that could emerge as a better alternate to physical and chemical syntheses of AgNPs. The development of fungi-mediated AgNPs can overcome MDR bacteria, especially *cmm* subsp. *michiganensis* which is responsible for the bacterial canker of tomato. However, further studies are required to assess the toxicity level and possible side effects that may arise from the penetration ability of AgNPs.

Data Availability

The data used to support the findings of this study are included within the article.

Conflicts of Interest

The authors declare no conflict of interest.

Acknowledgments

The authors are grateful to Lund University, Sweden, the Higher Education Commission-Pakistan, and the "Atomic Resolution Cluster"—a Research Infrastructure Fellow program of the Swedish Foundation for Strategic Research. I duly acknowledge Sven Lidin for providing the PXRD lab facility.

References

[1] J. O. W. González, N. Stefanazzi, A. P. Murray, A. A. Ferrero, and B. F. Band, "Novel nanoinsecticides based on essential oils to control the German cockroach," *Journal of Pest Science*, vol. 88, no. 2, pp. 393–404, 2015.

[2] H. Chhipa and P. Joshi, "Nanofertilisers, nanopesticides and nanosensors in agriculture," in *Nanoscience in Food and Agriculture 1*, S. Ranjan, N. Dasgupta, and E. Lichtfouse, Eds., pp. 247–282, Springer, Champ, 2016.

[3] P. L. Kashyap, X. Xiang, and P. Heiden, "Chitosan nanoparticle based delivery systems for sustainable agriculture," *International Journal of Biological Macromolecules*, vol. 77, pp. 36–51, 2015.

[4] I. C. Hwang, T. H. Kim, S. H. Bang et al., "Insecticidal effect of controlled release formulations of etofenprox based on nanobio technique," *Journal of the Faculty of Agriculture, Kyushu University*, vol. 56, no. 1, pp. 33–40, 2011.

[5] J. J. Kim, "Nano silver chemotherapeutic agents and its applications," *International Journal of Chemical Engineering*, vol. 22, pp. 655–660, 2004.

[6] H. P. Borase, B. K. Salunke, R. B. Salunkhe et al., "Plant extract: a promising biomatrix for ecofriendly, controlled synthesis of silver nanoparticles," *Applied Biochemistry and Biotechnology*, vol. 173, no. 1, pp. 1–29, 2014.

[7] D. S. Balaji, S. Basavaraja, R. Deshpande, D. B. Mahesh, B. K. Prabhakar, and A. Venkataraman, "Extracellular biosynthesis of functionalized silver nanoparticles by strains of *Cladosporium cladosporioides* fungus," *Colloids and Surfaces B: Biointerfaces*, vol. 68, no. 1, pp. 88–92, 2009.

[8] A. K. Gade, P. Bonde, A. P. Ingle, P. D. Marcato, N. Durán, and M. K. Rai, "Exploitation of *Aspergillus niger* for synthesis of silver nanoparticles," *Journal of Biobased Materials and Bioenergy*, vol. 2, no. 3, pp. 243–247, 2008.

[9] A. Ingle, A. Gade, S. Pierrat, C. Sonnichsen, and M. Rai, "Mycosynthesis of silver nanoparticles using the fungus *Fusarium acuminatum* and its activity against some human pathogenic bacteria," *Current Nanoscience*, vol. 4, no. 2, pp. 141–144, 2008.

[10] S. U. Picoli, M. Durán, P. F. Andrade, and N. Duran, "Silver nanoparticles/silver chloride (Ag/AgCl) synthesized from *Fusarium oxysporum* acting against *Klebsiella pneumouniae* carbapenemase (KPC) and extended spectrum beta-lactamase (ESBL)," *Frontiers in Nanoscience and Nanotechnology*, vol. 2, no. 2, pp. 107–110, 2016.

[11] A. Noshad, M. Iqbal, L. Folkers et al., "Antibacterial effect of silver nanoparticles (AgNPs) synthesized from Trichoderma harzianum against Clavibacter michiganensis," *Journal of Nano Research*, vol. 58, pp. 10–19, 2019.

[12] V. Rathod, A. Banu, and E. Ranganath, "Biosynthesis of highly stabilized silver nanoparticles by *Rhizopus stolonifer* and their anti-fungal efficacy," *International Journal of Pharmacy and Biomedical Sciences*, vol. 2, no. 1, pp. 241–245, 2012.

[13] S. Honary, H. Barabadi, E. Gharaei-Fathabad, and F. Naghibi, "Green synthesis of copper oxide nanoparticles using *Penicillium aurantiogriseum*, *Penicillium citrinum* and *Penicillium waksmanii*," *Digest Journal of Nanomaterials and Biostructures*, vol. 7, no. 3, pp. 999–1005, 2012.

[14] M. El-Rafie, A. A. Mohamed, T. I. Shaheen, and A. Hebeish, "Antimicrobial effect of silver nanoparticles produced by fungal process on cotton fabrics," *Carbohydrate Polymers*, vol. 80, no. 3, pp. 779–782, 2010.

[15] A. Noshad, A. Noshad, M. Iqbal et al., "Aphidicidal potential of ethyl acetate extract from Pleurotus ostreatus," *Sarhad Journal of Agriculture*, vol. 31, no. 2, pp. 101–105, 2015.

[16] M. Gajbhiye, J. Kesharwani, A. Ingle, A. Gade, and M. Rai, "Fungus-mediated synthesis of silver nanoparticles and their activity against pathogenic fungi in combination with fluconazole," *Nanomedicine: Nanotechnology, Biology and Medicine*, vol. 5, no. 4, pp. 382–386, 2009.

[17] V. C. Verma, R. N. Kharwar, and A. Gange, "Biosynthesis of antimicrobial silver nanoparticles by the endophytic fungus *Aspergillus clavatus*," vol. 5, no. 1, pp. 33–40, 2010.

[18] Y. Qian, H. Yu, D. He et al., "Biosynthesis of silver nanoparticles by the endophytic fungus *Epicoccum nigrum* and their activity against pathogenic fungi," *Bioprocess and Biosystems Engineering*, vol. 36, no. 11, pp. 1613–1619, 2013.

[19] D. Singh, V. Rathod, S. Ninganagouda, J. Hiremath, A. K. Singh, and J. Mathew, "Optimization and characterization of silver nanoparticle by endophytic fungi *Penicillium* sp. isolated from *Curcuma longa* (turmeric) and application studies against MDR *E. coli* and S. *aureus*," *Bioinorganic Chemistry and Applications*, vol. 2014, Article ID 408021, 8 pages, 2014.

[20] D. L. Strider, "Bacterial canker of tomato caused by Corynebacterium michiganense; a literature review and bibliography," *North Carolina Agricultural Experiment Station Bulletin*, 1969.

[21] M. J. Davis, A. G. Gillaspie, A. K. Vidaver, and R. W. Harris, "*Clavibacter:* a new genus containing some phytopathogenic coryneform bacteria, including *Clavibacter xyli* subsp. *xyli* sp. nov., subsp. nov. and *Clavibacter xyli* subsp. *cynodontis* subsp. nov., pathogens that cause ratoon stunting disease of sugarcane and bermudagrass stunting disease," *International Journal of Systematic Bacteriology*, vol. 34, no. 2, pp. 107–117, 1984.

[22] M. E. Rateb, I. Hallyburton, W. E. Houssen et al., "Induction of diverse secondary metabolites in *Aspergillus fumigatus* by microbial co-culture," *RSC Advances*, vol. 3, no. 34, pp. 14444–14450, 2013.

[23] S. Sunkar and C. V. Nachiyar, "Biogenesis of antibacterial silver nanoparticles using the endophytic bacterium *Bacillus cereus* isolated from *Garcinia xanthochymus*," *Asian Pacific Journal of Tropical Biomedicine*, vol. 2, no. 12, pp. 953–959, 2012.

[24] K. Vahabi, G. A. Mansoori, and S. J. I. J. Karimi, "Biosynthesis of silver nanoparticles by fungus Trichoderma reesei (a route for large-scale production of AgNPs)," *Insciences Journal*, vol. 1, no. 1, pp. 65–79, 2011.

[25] J.-c. Qu, Y. P. Chang, Y. H. Ma et al., "A simple and sensitive colorimetric method for the determination of propafenone by silver nanoprobe," *Sensors and Actuators B: Chemical*, vol. 174, pp. 133–139, 2012.

[26] M. K. Alqadi, O. A. A. Noqtah, F. Y. Alzoubi, J. Alzouby, and K. Aljarrah, "pH effect on the aggregation of silver nanoparticles synthesized by chemical reduction," *Materials Science-Poland*, vol. 32, no. 1, pp. 107–111, 2014.

[27] K. Zomorodian, S. Pourshahid, A. Sadatsharifi et al., "Biosynthesis and characterization of silver nanoparticles by *Aspergillus* species," *BioMed Research International*, vol. 2016, Article ID 5435397, 6 pages, 2016.

[28] V. Petříček, M. Dušek, and L. Palatinus, "Crystallographic computing system JANA2006: general features," *Zeitschrift für Kristallographie - Crystalline Materials*, vol. 229, no. 5, pp. 345–352, 2014.

[29] X. Zhong, Y. Song, P. Yang et al., "Titanium surface priming with phase-transited lysozyme to establish a silver nanoparticle-loaded chitosan/hyaluronic acid antibacterial multilayer via layer-by-layer self-assembly," vol. 11, no. 1, Article ID e0146957, 2016.

[30] J.-C. Jin, X. J. Wu, J. Xu, B. B. Wang, F. L. Jiang, and Y. Liu, "Ultrasmall silver nanoclusters: Highly efficient antibacterial activity and their mechanisms," *Biomaterials Science*, vol. 5, no. 2, pp. 247–257, 2017.

[31] P. C. Lombardo, A. L. Poli, L. F. Castro, J. R. Perussi, and C. C. Schmitt, "Photochemical deposition of silver nanoparticles on clays and exploring their antibacterial activity," *ACS Applied Materials & Interfaces*, vol. 8, no. 33, pp. 21640–21647, 2016.

[32] T. Kim, G. B. Braun, Z. G. She, S. Hussain, E. Ruoslahti, and M. J. Sailor, "Composite Porous silicon–silver nanoparticles as theranostic antibacterial agents," *ACS Applied Materials & Interfaces*, vol. 8, no. 44, pp. 30449–30457, 2016.

[33] K. Zawadzka, K. Kądzioła, A. Felczak et al., "Surface area or diameter – which factor really determines the antibacterial activity of silver nanoparticles grown on TiO2coatings?," *New Journal Chemistry*, vol. 38, no. 7, pp. 3275–3281, 2014.

[34] U. Klueh, V. Wagner, S. Kelly, A. Johnson, and J. D. Bryers, "Efficacy of silver-coated fabric to prevent bacterial colonization and subsequent device-based biofilm formation," *Journal of Biomedical Materials Research*, vol. 53, no. 6, pp. 621–631, 2000.

[35] A. Parveen and S. Rao, "Effect of nanosilver on seed germination and seedling growth in *Pennisetum glaucum*," *Journal of Cluster Science*, vol. 26, no. 3, pp. 693–701, 2015.

[36] G. de la Rosa, M. L. López-Moreno, D. de Haro, C. E. Botez, J. R. Peralta-Videa, and J. L. Gardea-Torresdey, "Effects of ZnO nanoparticles in alfalfa, tomato, and cucumber at the germination stage: root development and X-ray absorption spectroscopy studies," *Pure and Applied Chemistry*, vol. 85, no. 12, pp. 2161–2174, 2013.

[37] A. K. Shaw and Z. J. C. Hossain, "Impact of nano-CuO stress on rice (*Oryza sativa* L.) seedlings," *Chemosphere*, vol. 93, no. 6, pp. 906–915, 2013.

[38] Z. Wang, X. Xie, J. Zhao et al., "Xylem- and phloem-based transport of cuo nanoparticles in maize (*Zea mays* L.)," vol. 46, no. 8, pp. 4434–4441, 2012.

[39] C. Srinivasan and R. Saraswathi, "Nano-agriculture—carbon nanotubes enhance tomato seed germination and plant growth," *Current science*, vol. 99, no. 3, pp. 274-275, 2010.

[40] J. Yasur and P. U. Rani, "Environmental effects of nanosilver: impact on castor seed germination, seedling growth, and plant

physiology," *Environmental Science and Pollution Research*, vol. 20, no. 12, pp. 8636–8648, 2013.

[41] G. F. Webb, E. M. C. D'Agata, P. Magal, and S. Ruan, "A model of antibiotic-resistant bacterial epidemics in hospitals," *Proceedings of the National Academy of Sciences of the United States of America*, vol. 102, no. 37, pp. 13343–13348, 2005.

[42] C. G. Gemmell, D. I. Edwards, A. P. Fraise et al., "Guidelines for the prophylaxis and treatment of methicillin-resistant *Staphylococcus aureus* (MRSA) infections in the UK," *Journal of Antimicrobial Chemotherapy*, vol. 57, no. 4, pp. 589–608, 2006.